 FDMP, vol.3, no.4, pp.339-347, 2007

Effect of Large Eccentric Rotation on the Stability of Liquid Bridges

A. Laverón-Simavilla[1], V. Lapuerta[1], J. Rodríguez[1] and M. A. González[1]

Abstract: A cylindrical liquid bridge supported between two circular-shaped disks in isorotation is considered. The effect of an offset between the rotation axis and the axis of the two supporting disks (eccentricity) on the stability of the liquid bridge is investigated. In a previous work a numerical method used to determine the stability limit for different values of eccentricity was validated comparing these results with analytical and experimental results for small eccentricity values, recovering the same behavior. In this work we use the numerical method to extend the analysis to large values of the eccentricity, finding a change in the bifurcation diagrams. The evolution of stable and unstable shapes for different bifurcation curves is also compared.

Keyword: Liquid bridge; Microgravity; Stability.

1 Introduction

The behavior of liquid bridges has been widely studied, both theoretically and experimentally, due to the use of this configuration in fabricating ultrapure semiconductor crystals. In this technique, known as the floating zone technique [Amberg G. and Shiomi J., (2005), Gelfgat A.Yu., Rubinov A., Bar-Yoseph P.Z. and Solan A. (2005), Lan and Yeh B.C. (2005), Lappa (2005)], rotation of the supports is used to achieve a uniform temperature field. The first studies on static shapes of liquid bridges held between two coaxial disks dates back from the XIX century [Plateau (1863)]. The response of this configuration subjected to various disturbances has been extensively studied including the calculation of the equilibrium shapes and their stability limits.

[1] E.T.S.I.Aeronáuticos (Universidad Politécnica de Madrid), Madrid, Spain

Liquid bridges can be also used either as accelerometers for steady accelerations or as tensiometers. This can be done by fitting the theoretical predictions to the observed contours of the liquid bridges [Cabezas, Montanero, Acero, Jaramillo and Fernández (2002)].

In this paper a cylindrical liquid bridge supported between two circular-shaped disks in isorotation is considered. In the absence of gravity, two types of instability, namely, *C* mode and amphora mode, depending on the slenderness, can appear [Vega and Perales (1983); Perales, Sanz and Rivas (1990)].

In a previous work [Lapuerta, Laverón-Simavilla and Rodríguez (2007)] the effect of an offset between the rotation axis and the axis of the two supporting disks (eccentricity) on these stabilities was investigated. The stability limits and the equilibrium shapes of the configuration were calculated using an extension of an already implemented numerical method [Laverón-Simavilla and Perales (1995); Laverón-Simavilla and Checa (1997)].

The calculated stability limits were compared with the analytical results of Perales, Sanz and Rivas (1990) (only valid for small eccentricity values) recovering the same behavior for both amphora and C modes.

For the C mode, numerical results were also compared with the results of an experiment aboard TEXUS-23 (see Sanz, Perales and Rivas (1992)) recovering the stability limit and the equilibrium shapes.

In this work we extend the analysis to large values of eccentricity. The numerical method is used to find stable and unstable shapes and to determine the stability limit for different values of eccentricity, finding new behaviors of the stability diagrams not detected previously.

2 Problem Formulation

The fluid configuration consists of a liquid bridge as sketched in Fig. 1. The liquid column is held by surface tension forces between two disks of radiusR_0, placed a distance L apart.

Both disks are parallel and coaxial. The volume of the bridge is that corresponding to a cylindrical one, $V = \pi R_0^2 L$. The liquid and the disks are solidly rotating at an angular speed Ω around an axis which is parallel to the axis of the disks, and is placed a small distance E (eccentricity) apart from this line.

The equation governing the steady shape of the liquid bridge is obtained by expressing the equilibrium between the different forces at the interface

$$\sigma \tilde{M}(R) + \tilde{P} + \frac{1}{2}\rho\Omega^2 D^2 = 0 \tag{1}$$

where $R = R(Z,\theta)$ is the equation of the gas-liquid interface, σ is the surface tension, $\tilde{M}(R)$ is twice the mean curvature of the interface, $\tilde{P}$ is the pressure difference at the origin, ρ is the liquid density and D is the distance between a point of the free surface and the rotation axis (see Fig. 1) which, in terms of the shape of the surface and the azimuthal angle θ, can be calculated as:

$$D = \left(R^2 + 2ER\cos\theta + E^2\right)^{1/2} \tag{2}$$

Equation (1) has to be integrated with the boundary conditions

$$R(\pm L/2, \theta) = R_0 \tag{3}$$

$$R(Z,\theta) = R(Z,\theta + 2\pi) \tag{4}$$

$$\frac{1}{2}\int_{-L/2}^{L/2} dZ \int_0^{2\pi} R^2(Z,\theta)d\theta = \pi L R_0^2 \tag{5}$$

Eq. (3) indicates that the liquid column remains anchored to the disk edges, Eq. (4) comes from the azimuthal periodicity and Eq. (5) expresses the conservation of the volume of the liquid bridge.

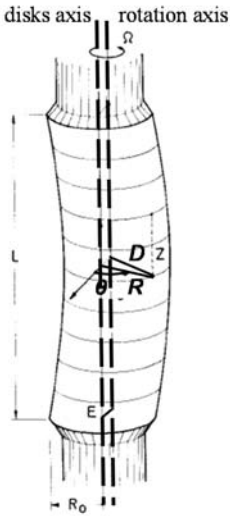

Figure 1: Geometry and coordinate system for the liquid bridge problem

Let us introduce the following dimensionless variables and parameters

$$\Lambda = L/2R_0, \quad e = E/R_0, \quad W = \rho\Omega^2 R_0^3/\sigma,$$
$$P = \tilde{P}R_0/\sigma, \quad z = Z/R_0, \quad F(z,\theta) = R(z,\theta)/R_0 \tag{6}$$

where $\Lambda$is the liquid bridge slenderness, e the dimensionless eccentricity, W the Weber number and $P$the dimensionless reference pressure.

The formulation of the problem in dimensionless variables becomes

$$M(F) + P + \frac{1}{2}W\left(F^2 + 2eF\cos\theta + e^2\right) = 0 \tag{7}$$

with

$$M(F) = \Big[F(1+F_z^2)(F_{\theta\theta} - F) + FF_{zz}(F^2 + F_\theta^2) - 2F_\theta(F_\theta + FF_zF_{\theta\theta})\Big] \Big/ \Big[\left(F^2(1+F_z^2) + F_\theta^2\right)^{3/2}\Big] \tag{8}$$

The dimensionless boundary conditions for Eq. (7) are

$$F(\pm\Lambda, \theta) = 1 \tag{9}$$

$$F(z,\theta) = F(z,\theta + 2\pi) \tag{10}$$

and

$$\int_{-\Lambda}^{\Lambda} dz \int_0^{2\pi} F^2(z,\theta)d\theta = 4\pi\Lambda \tag{11}$$

3 Numerical method

An algorithm, based on a continuation method [Keller (1987)] capable of over-passing bifurcation points and turning points (which appear for the amphora mode and the C mode, respectively) was developed using a finite-difference method [Laverón-Simavilla and Perales (1995)] and was used to obtain the bifurcation diagrams and equilibrium shapes of liquid bridges subjected to lateral acceleration and other effects. The stable or unstable character of each of the shapes is calculated to determine the position of the stability limit.

In this paper the system of equations (7)-(11) is solved by using an extension of that algorithm to liquid bridges rotating around an eccentric axis to study the effect of combined eccentricity and angular speed.

The method is based on linearizing Eqs. (7)-(11) around a known solution $(F_0(z,\theta),P_0)$ by seeking solutions of the form

$$F(z,\theta) = F_0(z,\theta) + f(z,\theta) + o\left(\left|\frac{f}{F_0}\right|\right)$$

$$P = P_0 + p + o\left(\left|\frac{p}{P_0}\right|\right)$$

where $|f/F_0| \ll 1$ and $|p/P_0| \ll 1$. The leading terms obtained from Eq. (7) result in an equation for $f(z,\theta)$

$$\tilde{O}^{-3/2}\left\{\tilde{A} + \left(\tilde{B} - \frac{3\tilde{A}\tilde{Q}}{2\tilde{O}}\right) f + \left(\tilde{C} - \frac{3\tilde{A}\tilde{S}}{2\tilde{O}}\right) f_z + \left(\tilde{D} - \frac{3\tilde{A}\tilde{T}}{2\tilde{O}}\right) f_\theta\right\} + \tilde{E} f_{zz} + \tilde{G} f_{\theta\theta} + \tilde{H} f_{z\theta} + P_0 + p + \frac{1}{2} W\left(e^2 + F_0^2 + 2F_0 f\right) + eW(F_0 + f)\cos\theta + \frac{1}{2} We^2 = 0 \quad (12)$$

where $\tilde{A}$, $\tilde{B}$, $\tilde{C}$, $\tilde{D}$, $\tilde{E}$, $\tilde{G}$, $\tilde{H}$, $\tilde{O}$, $\tilde{Q}$, $\tilde{S}$ and $\tilde{T}$ are known functions of $F_0(z,\theta)$ and P_0 and consequently of the considered point on the interface. The leading terms obtained for the boundary conditions are

$$f(z,\theta) = f(z,\theta+2\pi) \quad (13)$$

$$F_0(\pm\Lambda,\theta) + f(\pm\Lambda,\theta) = 0 \quad (14)$$

and

$$\int_{-\Lambda}^{\Lambda} \mathrm{d}z \int_0^{2\pi} F_0(z,\theta)^2 \mathrm{d}\theta + 2\int_{-\Lambda}^{\Lambda} \mathrm{d}z \int_0^{2\pi} [F_0(z,\theta) f(z,\theta)]\,\mathrm{d}\theta = 4\pi\Lambda \quad (15)$$

If $(F_0(z,\theta),P_0)$ were an exact solution of the problem, Eqs. (12)-(15) could have been simplified, but all the terms have been retained because $(F_0(z,\theta),P_0)$ will only be an approximation to the solution in the iterative scheme.

In order to develop a center finite difference scheme the domain has been characterized by a mesh, defined as the intersection of the free surface with the following planes:

$$z = \Lambda\left(\frac{2j}{J} - 1\right), \quad j = 0,1,\ldots,J \quad (16)$$

and

$$\theta = \frac{2\pi}{I+1} i, \quad i = 0,1,\ldots,I \quad (17)$$

By doing so, the system (12)-(15) yield a linearized finite-difference equation system which can be written as follows:

$$\alpha_{ij} f_j^i + \beta_{ij} f_{j-1}^i + \gamma_{ij} f_{j+1}^i + \delta_{ij} f_j^{i-1} + \varphi_{ij} f_j^{i+1} + \phi_{ij}\left(f_{j+1}^{i+1} - f_{j+1}^{i-1} - f_{j-1}^{i+1} + f_{j-1}^{i-1}\right) + p = \psi_{ij}, \quad i = 0,\ldots,I, \quad j = 0,\ldots,J \quad (18)$$

$$f_j^0 - f_j^{I+1} = 0, \quad j = 0,\ldots,J \quad (19)$$

$$f_J^i = 1 - F_{0,J}^i, \quad i = 0,\ldots,I \quad (20)$$

$$f_0^i = 1 - F_{0,0}^i, \quad i = 0,\ldots,I \quad (21)$$

$$\sum_{i=0}^{I}\sum_{j=0}^{J} a_{ij} f_j^i = A \quad (22)$$

where the coefficients α_{ij}, β_{ij}, γ_{ij}, δ_{ij}, φ_{ij}, ϕ_{ij} , ψ_{ij}, a_{ij} and A are functions of the values $F_{0,j}^i$ and P_0.

If no further modifications were made, the algorithm would destabilize when crossing any critical point. To stabilize the algorithm a new equation defining the arc-length parameter needs to be included. The details of the numerical method used to locate bifurcation and limit points are identical to those outlined elsewhere [Laverón-Simavilla and Perales (1995)] and will not be repeated here.

4 Results

First, let us summarize some analytical results obtained by Vega and Perales (1983) later extended by Perales, Sanz and Rivas. (1990) (the results are only valid for small eccentricity). They looked for a solution of Eqs. (7) to (11) for e=0 of the form: $F = 1 + \varepsilon f + o(\varepsilon)$, $P = 1 - W/2 + \varepsilon p + o(\varepsilon)$, $\varepsilon \ll 1$ (small departures from a cylindrical liquid bridge), finding the non-zero solutions:

(i) Non axisymmetric shapes (C-mode)

$$W_0 = \left(\frac{\pi}{2\Lambda}\right)^2, \quad f = \cos\theta \cos\left(\frac{\pi}{2\Lambda} z\right), \quad p = 0 \tag{23}$$

(ii) Axisymmetric shapes (amphora mode)

$$W_0 = \left(\frac{\pi}{\Lambda}\right)^2 - 1, \quad f = \sin\left(\frac{\pi}{\Lambda} z\right), \quad p = 0 \tag{24}$$

The functions $W_0(\Lambda)$ represent in the $\Lambda - W$ plane the curves where the transition between stable and unstable equilibrium shapes appears. These two curves have been plotted in Fig. 2. The point B, for which expressions (23) and (24) are equal ($\Lambda = \sqrt{3}\pi/2$), marks the transition between the C and the amphora mode breakage.

For e=0 the bifurcation diagrams for both C and amphora mode are as the ones sketched in Figs. 3(a) and 3(b), that is, the bifurcation is subcritical. Thus, both equilibrium shapes (C-mode shapes and amphora mode shapes) are always unstable. If the value of the rotation speed is slowly increased starting from zero, stable cylindrical shapes are obtained until W reaches W_0, at which point a breaking process appears. Thus, for e=0 liquid bridges with $\Lambda < \sqrt{3}\pi/2$ loose stability with non-axisymmetric breakage and liquid bridges with $\Lambda > \sqrt{3}\pi/2$ loose stability with axisymmetric breakage.

In the following we describe the influence of combined eccentricity and angular speed. For the C-mode the bifurcation equation obtained from the analytical model with $e \ll 1$ takes the form

$$W = W_0 + 3\phi_{300}^{1/3}(\Lambda)\left(\frac{\pi}{2\Lambda^2}\right)^{2/3} e^{2/3} + \ldots, \tag{25}$$

where $W_0(\Lambda)$ is given by Eq. (23) and $\phi_{300}(\Lambda) < 0$ is given in Perales, Sanz and Rivas (1990). This relationship has been sketched in Fig. 3(a). Thus, the effect of eccentricity for C-mode changes the character of the destabilization, because it is due to a turning point (for $e \neq 0$) instead of to a subcritical bifurcation point (for e=0).

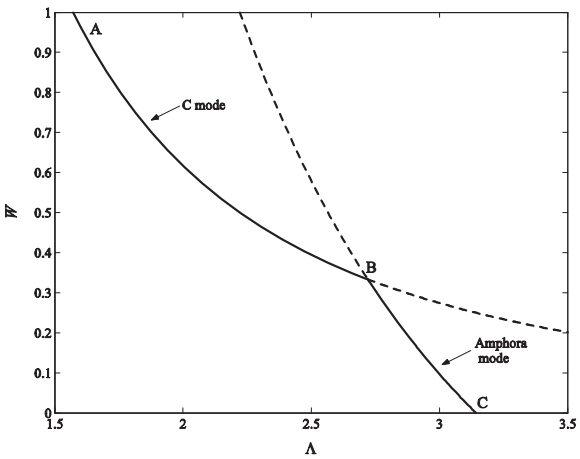

Figure 2: Stability diagram for zero eccentricity [Perales, Sanz and Rivas (1990)].

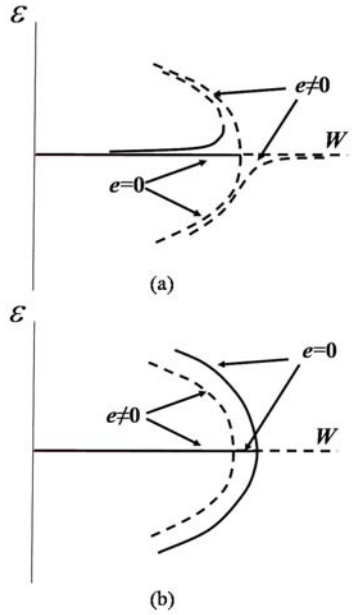

Figure 3: Bifurcation diagrams for (a) C-mode and (b) amphora mode [Perales, Sanz and Rivas (1990)]

For the amphora mode the bifurcation equation obtained from the analytical model with $e \ll 1$ takes the form

$$W = W_0(\Lambda) - \frac{\phi_{120}}{\phi_{101}} e^2 + \ldots, \tag{26}$$

where $W_0(\Lambda)$ is given by Eq. (24) and ϕ_{101} and ϕ_{120} are given in Perales et al. (1990). This relationship has been sketched in Fig. 3(b). Thus, the effect of the eccentricity for amphora mode does not change the character of the destabilization, as happens for the the C-mode, being always due to a subcritical bifurcation point.

With the numerical method we recovered the stability threshold for e=0, and we analyzed the dependency of this threshold on the eccentricity and the angular speed for $e \leq O(1)$ [Lapuerta, Laverón-Simavilla and Rodríguez] for both amphora and C-modes.

Here we extend the analysis to a wider range of parameters. This analysis has shown a more complex behaviour of the destabilization character for liquid bridges with $\Lambda < \sqrt{3}\pi/2$. Thus for a given liquid bridge, by increasing the eccentricity we have:

(i) A subcritical bifurcation point (for e=0).

(ii) A turning point (for $0 < e < e_c$).

(iii) A subcritical bifurcation point (for $e_c < e$).

Fig. 4 shows the critical value of the eccentricity e_c, for which the transition between cases (ii) and (iii) is encountered, as a function of the slenderness of the liquid bridge. The region corresponding to the turning point destabilization decreases as Λ increases, disappearing for $\Lambda = \sqrt{3}\pi/2$, for which the transition between C-mode to amphora mode for e=0 happens. For $e \ll 1$ the transition curve could be obtained by equating Eqs. (25) and (26).

Fig. 5 and 6 show the bifurcation diagrams obtained by representing the area of the section at z=0 and z=-Λ/2 respectively, as a function of W for Λ=2.7 and two values of eccentricity: e=0.08, which corresponds to the turning point character

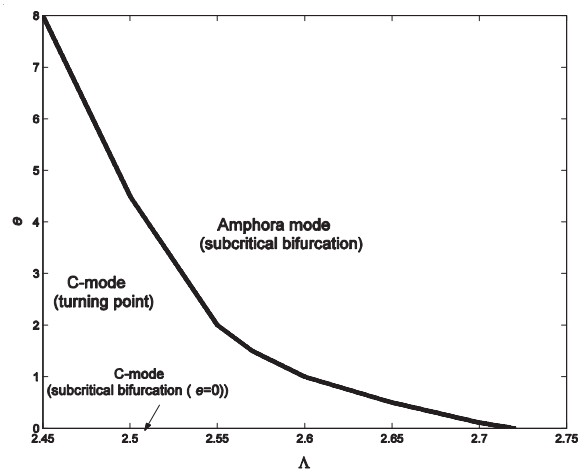

Figure 4: Transition curve between the subcritical bifurcation points and the turning points for the C-mode.

and e=0.7, which correspond to the subcritical bifurcation character. In the last case the bifurcation point appears for W=0.142070 and the turning point for W=0.143234. The stable part of the branches is represented with solid line, and the unstable part with dashed line.

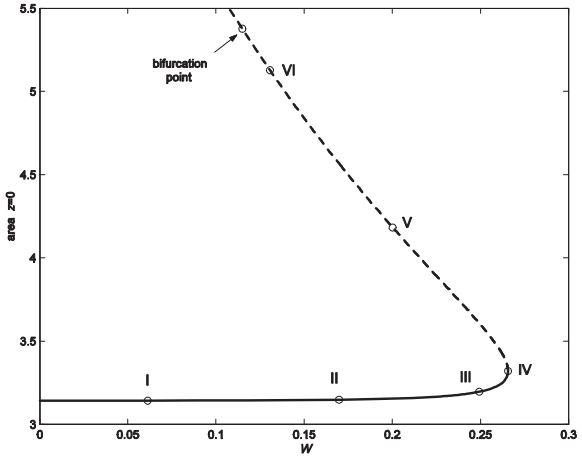

Figure 5: Bifurcation diagram for Λ=2.7 and e=0.08

Fig. 7 and 8 show the equilibrium shapes for the cases indicated in Fig.5 and 6 respectively. In Figure 8 equilibrium shapes for both, the main branch and the bifurcated one are represented.

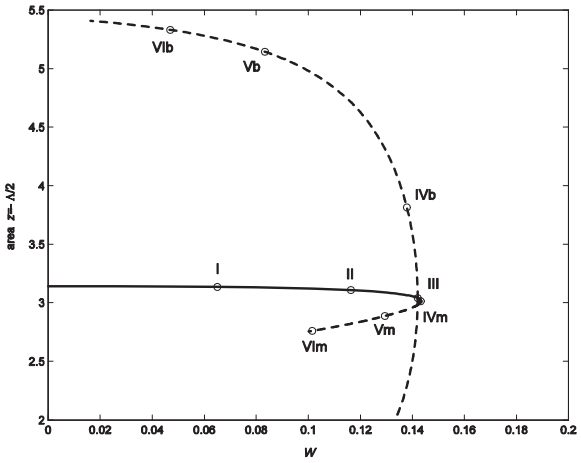

(a)

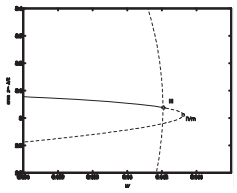

(b)

Figure 6: Bifurcation diagram for Λ=2.7 and e=0.7. Graphic (b) is a zoom of graphic (a) near de bifurcation point.

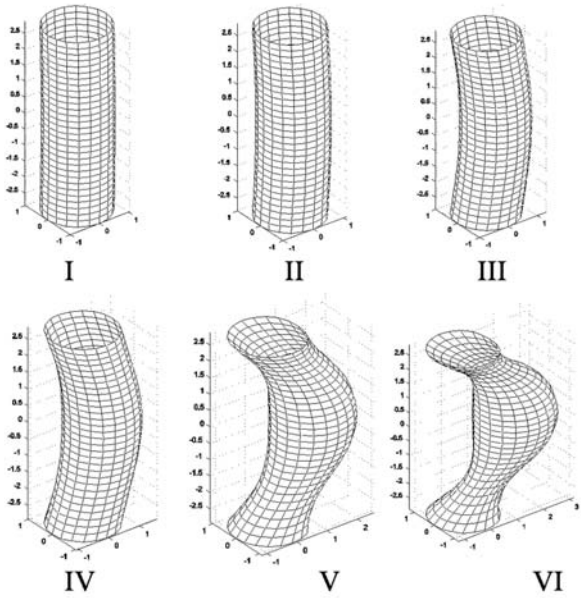

Figure 7: Evolution of the equilibrium shapes of a cylindrical liquid bridge with Λ=2.7 along the main branch for e=0.08. Shapes I to IV are stable and V and VI are unstable

As Figs. 7 and 8 show the behaviour of the equilibrium shapes for the bifurcation and turning points with $\Lambda < \sqrt{3}\pi/2$ is:

(i) For both bifurcation point with e=0 and turning point with $0 < e < e_c$ the associated eigenfunction is symmetric about the z=0 plane (that is, a C-mode) so that the breaking process will probably lead to a symmetric configuration.

(ii) For the subcritical bifurcation point with $e_c < e$ the associated eigenfunction is antisymmetric about the z=0 plane (that is, an amphora-mode) so that the breaking process will probably lead to a nonsymmetric configuration.

For liquid bridges with $\Lambda > \sqrt{3}\pi/2$there is no change in the character of the destabilization for increasing eccentricity, being always a subcritical bifurcation with an associated amphora mode.

Figure 9 shows the difference on the stability threshold for different values of e. The dot line marks the change of the destabilization character from C-mode to amphora mode. The region of the amphora mode destabilization increases for increasing eccentricity.

Fig. 10 shows the variation of the stability threshold as $W(\Lambda,e)$ for both C and amphora modes. The analysis shows that an increase of the eccentricity or the slenderness decreases the stability region,

Fig. 11 compares the equilibrium shapes in the critic points (turning or bifurcation point) for two liquid bridges of slenderness Λ=2.0 and Λ=2.7 respectively, for increasing values of the eccentricity.

Liquid bridges with low slenderness withstand more deformation before the breaking than those with large slenderness. Equilibrium shapes (e) and (f) are very similar being the eccentricity a lot larger in (f). The reason why is because in both cases the breaking is by an amphora mode, which is not the case of (b) and (c).

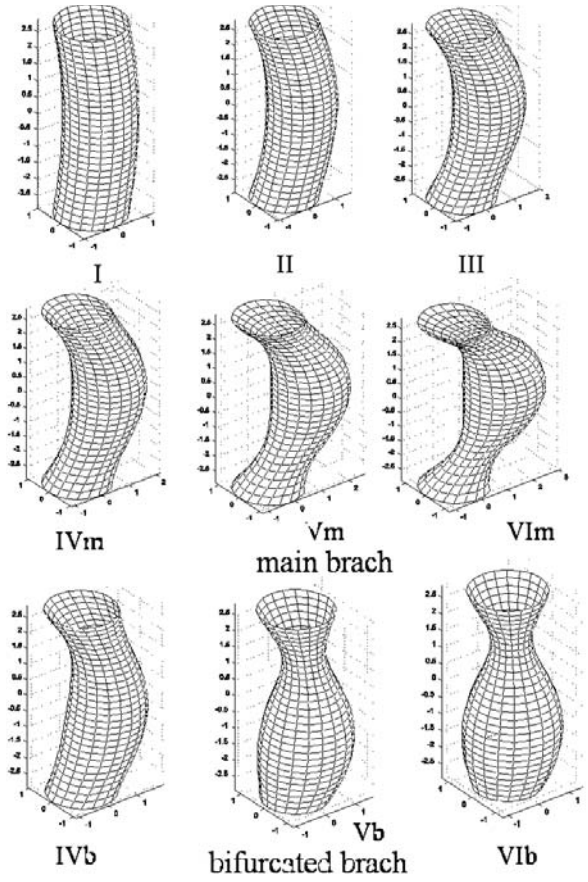

Figure 8: Evolution of the equilibrium shapes of a cylindrical liquid bridge with Λ=2.7 along the main branch of solution and the bifurcated one for e=0.7. Shapes I to III are stable and the rest are unstable

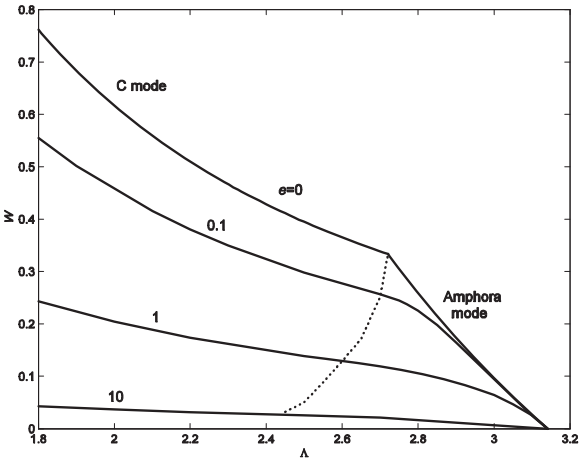

Figure 9: Comparison of the stability threshold for different values of e

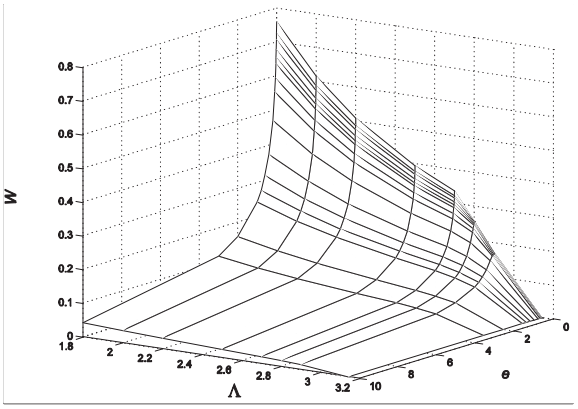

Figure 10: Combined effect of the slenderness and the eccentricity on the threshold stability

Although the numerical method presented here has been widely validated for other configurations, and in this one for small values of the eccentricity, with both theoretical and experimental results, a last validation has been done for large eccentricity, using the code Surface Evolver [Brakke (1992)]. In this code the surface is discretized using triangular elements. The user defines an initial surface and the Surface Evolver evolves it toward minimal energy by a gradient descent method. For the case presented here the energy is a combination of the surface tension and rotation energy.. The evolution of a liquid bridge with Λ=2 and e=10 for increasing Weber values using the Surface Evolver predicts the stability limit at W=0.21 and the numerical method used in this article at W=0.2. The agreement of the Weber value at the stability threshold is good. It has to be pointed out that only stable equilibrium shapes can be obtained from the Surface Evolver, bridges above the stability limit break and no equilibrium shapes can be found; the energy has a cusp point in the stability limit. The critical value of the parameter is found where the Evolver iteration diverges.

5 Conclusions

The stability limits of liquid bridges rotating around an eccentric axis are calculated numerically for large values of the eccentricity. The numerical method is used to find stable and unstable shapes and to determine the dependency of the

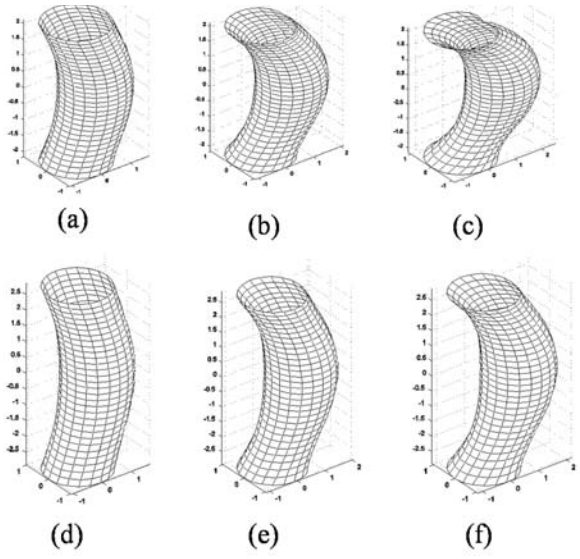

Figure 11: Equilibrium shapes at the stability threshold for Λ=2 and (a) e=0.1, (b) e=1, (c) e=10; $\Lambda = 2.7$ and (d) e=0.1, (e) e=1, (f) e=10.

stability threshold on the slenderness and eccentricity.

For both, amphora and C mode, the analysis shows that the stability region decreases, that is, the stability threshold occurs at lower values of the angular speed, as slenderness or eccentricity increase.

Liquid bridges with $\Lambda < \sqrt{3}\pi/2$ have a more complex destabilization character than those with $\Lambda > \sqrt{3}\pi/2$. Thus for a liquid bridge with $\Lambda < \sqrt{3}\pi/2$, by increasing the eccentricity value there is:

(i) A subcritical bifurcation point (for e=0) whose associated eigenfunction is symmetric about the z=0 plane (that is, a C-mode).

(ii) A turning point (for $0< e < e_c$) whose associated eigenfunction is a C-mode.

(iii) A subcritical bifurcation point (for $e_c < e$) which associated eigenfunction is antisymmetric about the z=0 plane (that is, an amphora mode).

For liquid bridges with $\Lambda > \sqrt{3}\pi/2$, there is no change in the character of the destabilization for increasing values of the eccentricity, being always a subcritical bifurcation with an associated amphora mode.

The region of the amphora mode destabilization increases for increasing values of the eccentricity.

Acknowledgement: This work has been sponsored by the Ministerio de Educación y Ciencia (MEC) and is part of a more general endeavor for the study of fluid physics in processing under microgravity (Proyect No. ESP2006-13030-C06-05)

References

Amberg G.; Shiomi J. (2005): Thermocapillary flow and phase change in some widespread materials processes, *FDMP: Fluid Dynamics and Materials Processing*, Vol. 1, pp. 81-95.

Brakke, K. (1992): The surface evolver, *Experimental Math*, Vol. 1, pp. 141.

Cabezas, G.; Montanero, J. M.; Acero, J.; Jaramillo, M. A.; Fernández, J. A. (2002): Detection of liquid bridge contours and its applications, *Measurement Science and Technology*, Vol. 13, pp. 829-835.

Gelfgat A.Yu.; Rubinov A.; Bar-Yoseph P.Z.; Solan A. (2005): On the Three-Dimensional Instability of Thermocapillary Convection in Arbitrarily Heated Floating Zones in Microgravity Environment, *FDMP: Fluid Dynamics and Materials Processing*, Vol. 1, pp. 21-32.

Keller, H. B. (1987): *Lectures on Numerical Methods in Bifurcation Problems*, Springer-Verlag, Berlin.

Lan C. W.; Yeh B. C. (2005), Effects of rotation on heat flow, segregation, and zone shape in a small-scale floating-zone silicon growth under axial and transversal magnetic fields, *FDMP: Fluid Dynamics and Materials Processing*, Vol. 1, pp. 33-44.

Lappa, M. (2005): Review: Possible strategies for the control and stabilization of Marangoni flow in laterally heated floating zones, *FDMP: Fluid Dynamics and Materials Processing*, Vol. 1, pp. 171-187.

Lapuerta, V., Laverón-Simavilla; A.; Ro-

dríguez, J. (2007): Stability of liquid bridges subject to an eccentric rotation, *Advances in Space Research* (under review).

Laverón-Simavilla; A., Checa, E. (1997): Effect of a lateral gravitational field on the non axisymmetric equilibrium shapes of liquid bridges held between eccentric disks and of volumes equal to those of cylinders, *Phys. Fluids*, Vol. 9, pp. 817.

Laverón-Simavilla; A., Perales, J. M. (1995): Equilibrium shapes of nonaxisymmetric liquid bridges of arbitrary volume in gravitational fields and their potential energy, *Phys. Fluids*, Vol. 7, pp. 1204-1213.

Perales, J. M.; Sanz, A.; Rivas, D. (1990): Eccentric Rotation of a Liquid Bridge, *Appl. Microgravity Tech. II*, Vol. 4, pp. 193-197.

Plateau, J. A. F. (1863): Experimental and theoretical researches on the figures of equilibrium of a liquid mass withdrawn from the action of gravity, translated in the *Annual Report of the Smithsonian Institute*, 1863-1866, pp. 207.

Sanz, A.; Perales, J.M.; Rivas, D. (1992): Rotational Instability of a Long Liquid Column, *ESA SP-1132*, Vol. 2, pp 8-21.

Vega, J. M.; Perales, J. M. (1983): Almost cylindrical isorotating liquid bridges for small bond number, *ESA SP-191*, ESA, Paris, pp. 247-252.